

**Mitochondrial transfer from bone marrow-derived stromal cells to pulmonary alveoli
protects against acute lung injury**

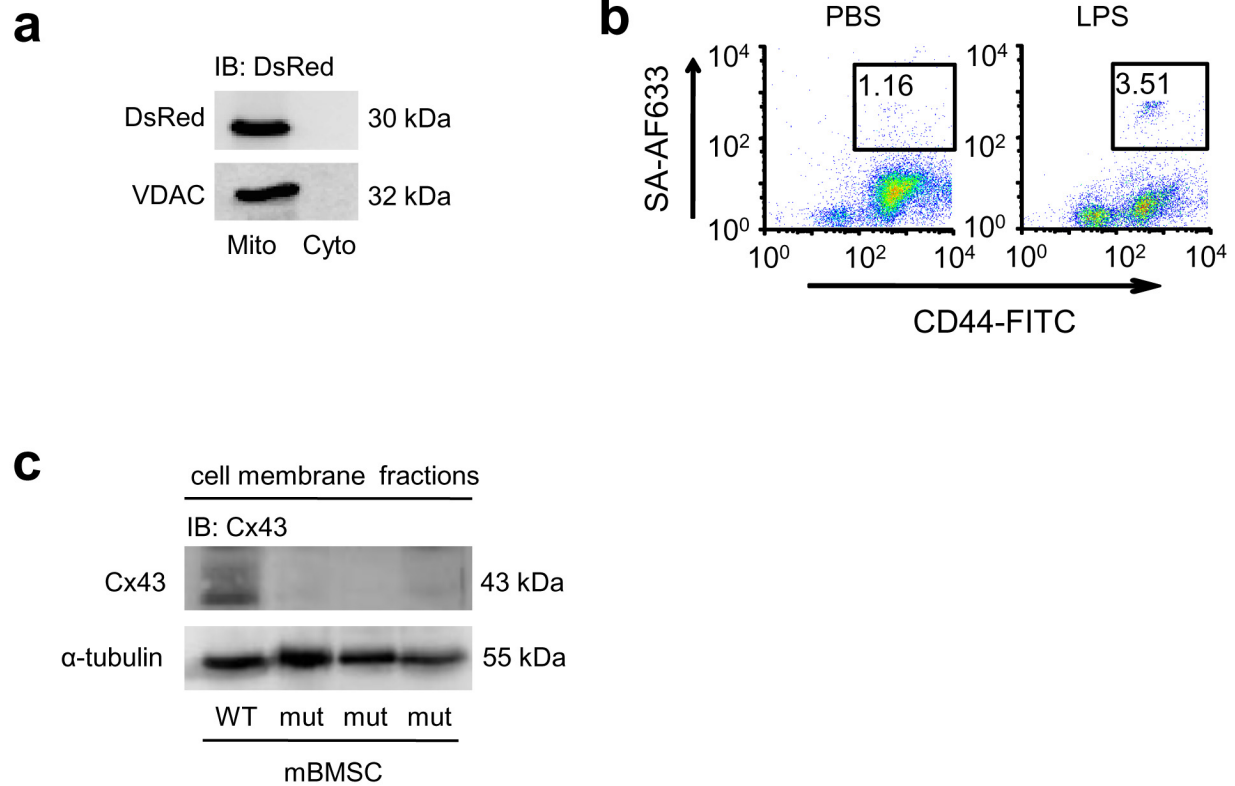
Mohammad Naimul Islam, Shonit R. Das, Memet T. Emin, Michelle Wei, Li Sun, Kristin Westphalen, David J. Rowlands, Sadiqa K. Quadri, Sunita Bhattacharya and Jahar Bhattacharya¹

Lung Biology Laboratory, Division of Pulmonary, Allergy & Critical Care Medicine, Department of Medicine, Columbia University, College of Physicians & Surgeons, New York, NY 10032, USA.

¹Corresponding author:

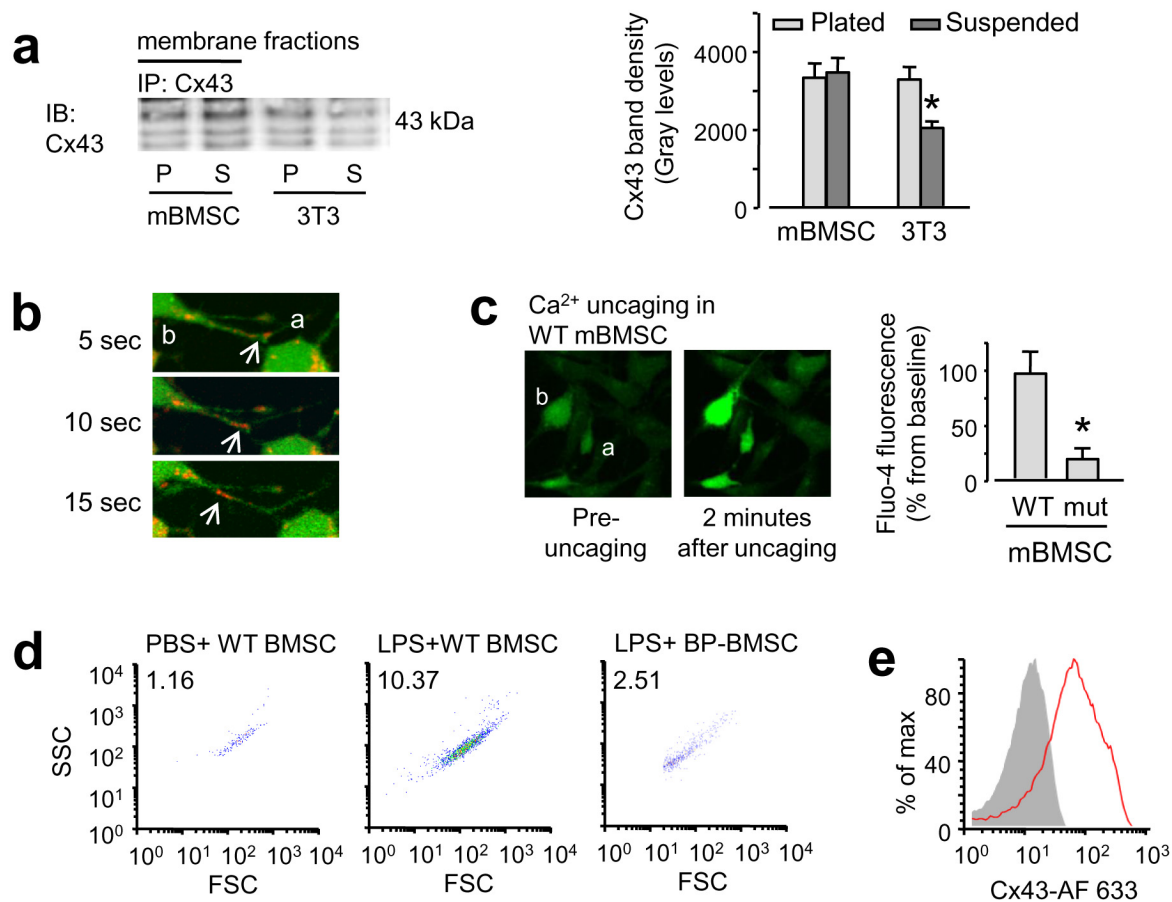
Jahar Bhattacharya, MD, DPhil
630 West 168th Street
BB 17-1705
New York, NY 10032
Phone: 212-305-7093
FAX: 212-305-6701
Email: jb39@columbia.edu

Supplementary figure 1



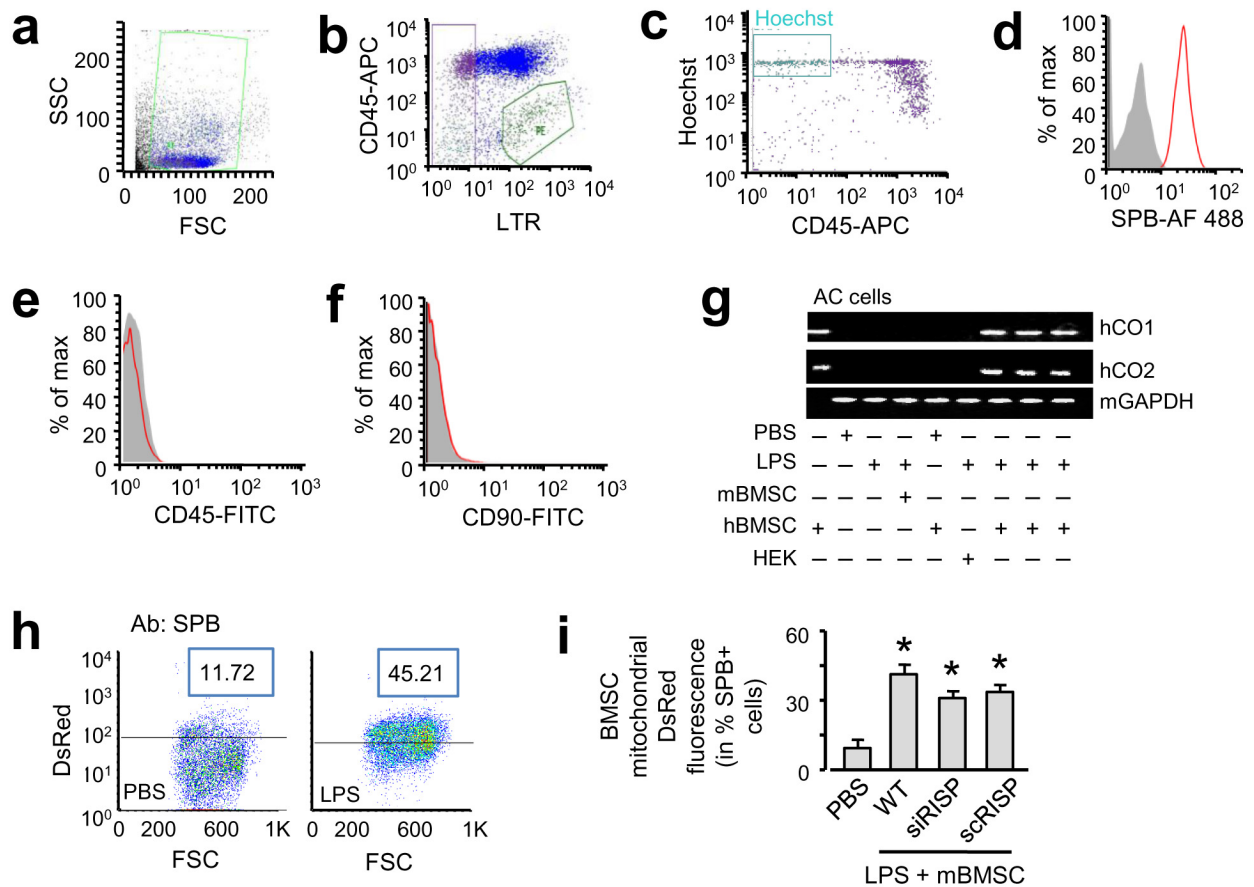
Supplementary Figure 1. Protein expressions in mBMSCs. (a) Gels show immunoblots on mitochondrial (*Mito*) and cytosolic (*Cyto*) fractions of mBMSC lysates. *Repeated 3 times.* (b) Quantification of lung mBMSCs by flow cytometry. mBMSCs were identified as cells positive for both streptavidin and the BMSC marker, CD44. Numbers are percent of total events analyzed. *Repeated 3 times.* (c) Gels show immunoblots of endogenous Cx43 on lysates of wild-type (*WT*) or mutant Cx43-expressing mBMSCs (*mut*). *Repeated 3 times.*

Supplementary figure 2



Supplementary Figure 2. Responses in cultured mBMSCs and in microvesicles recovered from the lung. (a) Gels show Cx43 immunoblots (*left*) and densitometry for the immunoblots (*right*). 3T3, mouse fibrocytes, *p*, plated; *s*, suspended. * $p < 0.05$ versus mBMSCs in suspension, *repeated 3 times*. (b) Confocal images show transfer of mBMSC mitochondria (red, *arrows*) through a nanotube. *Repeated 3 times*. (c) Images show cultured mBMSCs that were loaded with the Ca²⁺ cage, NP-EGTA and the Ca²⁺ dye, fluo-4. Ca²⁺ was uncaged from NP-EGTA in cell *b* (*left image*). Resulting increases of Ca²⁺ are shown in the right image both for the uncaged cell (*b*), as well as for an adjacent cell (*a*). Group data are changes in fluo-4 fluorescence in cells adjacent to the cells targeted for photolytic uncaging. WT, wild-type mBMSCs; *mut*, mutCx43-expressing mBMSCs. $n = 3$ monolayers for each bar. * $p < 0.05$ versus WT. (d) Plots show mitochondria-containing microvesicles (positive for DsRed) in lung supernatants 4 h after mBMSC instillation. Numbers are percent of total events analyzed. BP-BMSC, mBMSCs treated with the Ca²⁺ chelator, BAPTA-AM. *Repeated 3 times*. (e) Histograms show Cx43-stains on mBMSC-derived microvesicles. *Repeated 4 times*.

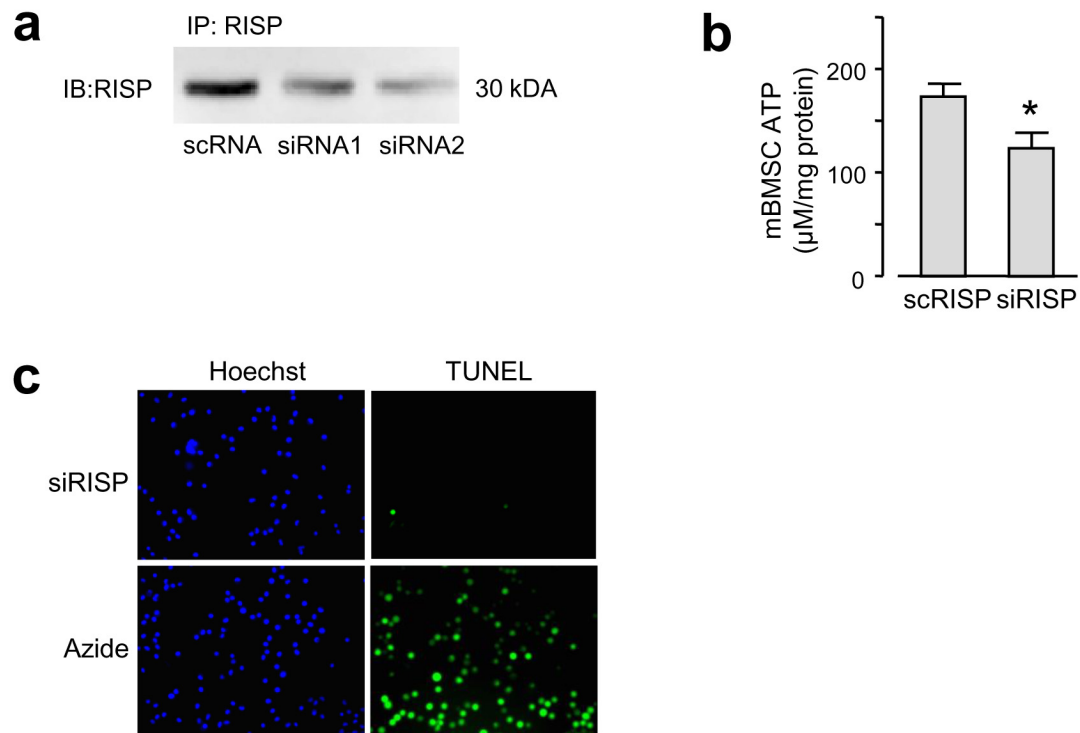
Supplementary figure 3



Supplementary Figure 3. Protein and mRNA analyses on primary epithelial isolates from lung.

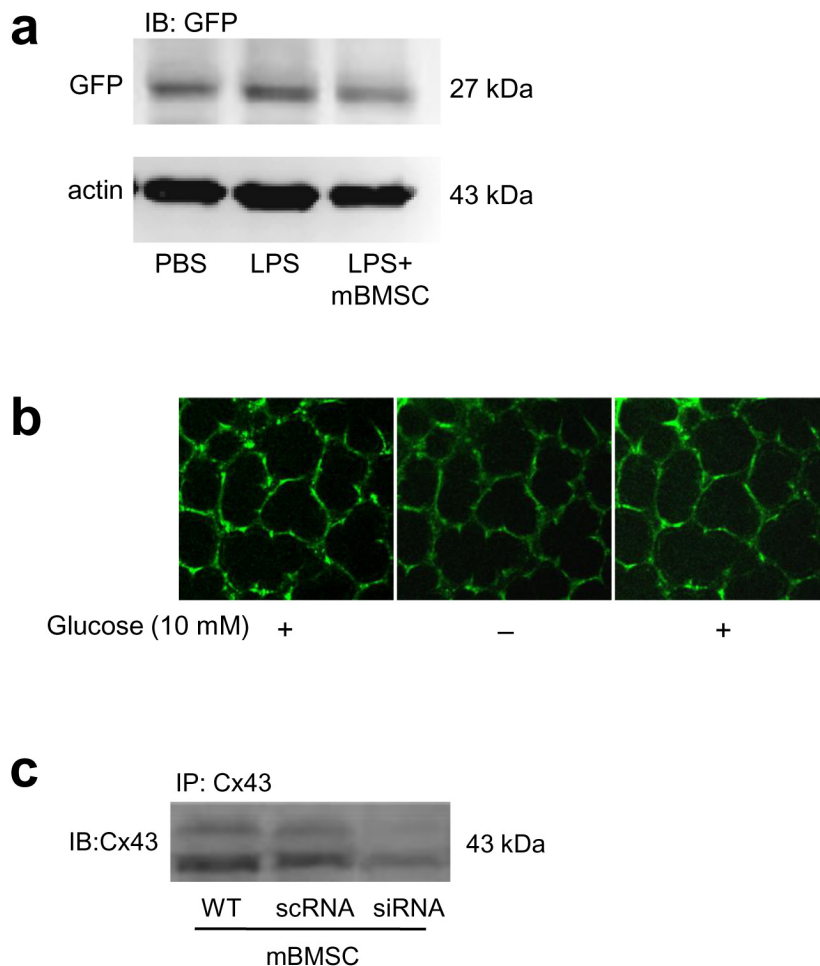
(a-c) Flow cytometry plots show the gating strategy for isolating alveolar epithelial cells. Cells were gated to exclude debris (a) and then analyzed for CD45 and lysotracker red (LTR) fluorescence (b). Cells negative for CD45 and positive for LTR (green in b) were collected. The LTR-negative cells (purple in b) were gated for Hoechst and CD45 fluorescence (c). Cells negative for both CD45 and LTR, but positive for Hoechst (cyan in c) were collected as a mixed cell population. (d-f) Histograms show that LTR-positive cell fractions were positive for SPB (d) and negative for CD45 (e) and mBMSC marker CD90 (f). Repeated 4 times. (g) Gels show amplified DNA sequences in isolated mixed alveolar cells (AC). *hCO1* and *hCO2*, human cytochrome oxidase 1 and 2; *hBMSC*, human BMSCs; *HEK*, human embryonic kidney cells; *mGAPdh*, mouse glyceraldehydes 3-phosphate dehydrogenase. Repeated 4 times. (h, i) Determinations in SPB-positive lung cells from single experiment (h) and group data (i). Numbers are percent DsRed positive events in SPB positive cells. Repeated 4 times. WT, wild-type; *siRISP*, mBMSCs treated with siRNA against Rieske iron-sulfur protein (RISP); *scrRISP*, mBMSCs treated with scrambled sequence of the siRNA against RISP. $n = 4$ lungs for each bar, * $p < 0.05$ versus PBS. There were no significant differences amongst the three bars on the right.

Supplementary figure 4



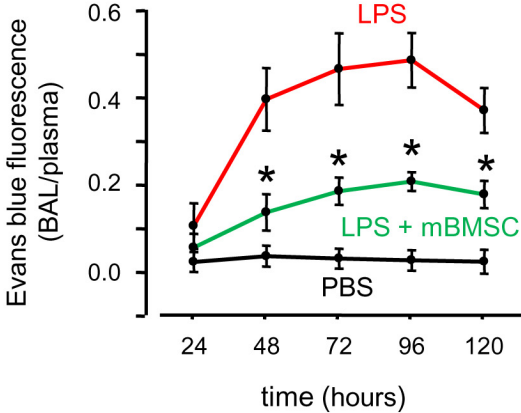
Supplementary Figure 4. Responses to RISP knockdown in mBMSCs. (a) Gels show immunoblots on mBMSC mitochondrial fractions. *RISP*, Rieske iron-sulfur protein; *siRNA*, small inhibitory RNA; *scRNA*, scrambled sequence of the siRNA. *Repeated 3 times*. (b) Group data are determinations in mBMSC lysates. *siRISP*, BMSCs treated with siRNA against RISP; *scRISP*, BMSCs treated with the scRNA. $n = 3$ monolayers for each bar, * $p < 0.05$ versus scRISP. (c) Images show mBMSC responses to RISP knockdown. *Repeated 3 times*.

Supplementary figure 5



Supplementary Figure 5. Perceval expression in the lung and Cx43 knockdown in mBMSCs. (a) Gels show immunoblots for GFP in lung lysates after indicated treatments. *Repeated 3 times.* (b) Confocal images show ATP fluorescence obtained sequentially at baseline, during glucose-containing lung perfusion (left), after a 1-hour perfusion with glucose-depleted buffer (middle) and then after 1 hour to glucose containing buffer (right). *Repeated 3 times.* (c) Gels show Cx43 expression after indicated treatments. *WT*, wild-type; *siRNA*, small-inhibitory RNA against Cx43; *scRNA*, scrambled sequence of the siRNA. *Repeated 3 times.*

Supplementary figure 6



Supplementary Figure 6. Alveolar leak in LPS lungs. Tracings show alveolar albumin leak after indicated treatments. BAL, bronchoalveolar lavage. $n = 4$ for each data point, * $p < 0.05$ versus LPS alone.

Supplementary methods

Reagents. We purchased Dulbecco's modified eagle medium (DMEM) and phosphate buffer saline (PBS) from Mediatech, fetal bovine serum (FBS), horse serum (HS) and bovine calf serum (BCS) from Hyclone, α -MEM (minimum essential medium), Opti-MEM, lipofectin and antibiotics (50 U ml⁻¹ penicillin G and 50 μ g ml⁻¹ streptomycin) and all fluorescent dyes, the Ca²⁺ chelator BAPTA-AM (1,2-bis(o-aminophenoxy)ethane-N,N,N',N'-tetraacetic acid, 40 μ M), biotin and streptavidin from Invitrogen, G418 from Calbiochem, and LPS (*E.coli*, 0111.B4), trypsin and α -glycyrrhetic acid (α -GA, 5 μ M) from Sigma. Dynasore (80 μ M) was a generous gift of Dr. Alice Prince (Columbia University). We purchased the peptide, gap 26 (VCYDKSFPISHVR; 160 μ M) and the scrambled peptide, scgapP26 (DRYVHFSVSPICK; 160 μ M) from Alpha Diagnostic International.

Antibodies. For flow cytometry experiments, we purchased fluorescence-tagged Abs against CD11b (Cat. # 17-4031), CD11c (Cat. # 12-0114), CD29 (Cat. # 17-0291), CD45 (Cat. # 11-0451 and 17-0451) from eBiosciences, Abs against CD54 (Cat. # 553252) and CD90 (Cat. # 551401) from BD Biosciences, and Ab against CD44 (Cat. # 53048) from Santa Cruz Biotechnology. For immunoblotting experiments, we purchased Abs against Cx43 from BD Biosciences (Cat. # 610061) and Santa Cruz Biotechnology (Cat. # 9059), Abs against surfactant protein B (SPB) (Cat. # 13978), Abs against voltage-dependent anion channel (VDAC) (Cat. # 8828) and GFP (Cat. # 9996) from Santa Cruz Biotechnology, Abs against Rieske iron-sulfur protein (RISP) from Molecular Probes (Cat. # 21346), Ab against DsRed (Cat. # 632496) from Clontech, Abs against actin (Cat. # 2066) and α -tubulin (Cat. # 9026) from Sigma. For immunoprecipitation and immunoblotting experiments, we diluted Abs against Cx43 (Santa Cruz), DsRed and VDAC as 1:250, Cx43 (BD) and RISP as 1:500, Abs against GFP and Actin as 1:1000 and Ab against α -tubulin as 1:2500.

Isolated, blood-perfused lungs. We excised lungs from anesthetized mice (i.p., Ketamine 80-100 mg kg⁻¹, Xylazine 1-5 mg kg⁻¹), then perfused with autologous blood through cannulas in the pulmonary artery and left atrium by our reported methods¹⁻³. We diluted the blood in 4% dextran (70 kDa), 1% fetal bovine serum and buffer (150 mmol l⁻¹ Na⁺, 5 mmol l⁻¹ K⁺, 1.0 mmol l⁻¹ Ca²⁺, 1 mmol l⁻¹ Mg²⁺, and 20 mmol l⁻¹ HEPES at pH 7.4) and maintained the perfusion flow rate at 0.5 ml min⁻¹ at 37 °C at osmolarity of mosM (Fiske Micro-Osmometer, Fiske® Associates), and hematocrit 10%. We inflated the lungs through a tracheal cannula with a gas mixture (30% O₂, 6% CO₂, balance N₂). Vascular (artery and vein at 10 and 3 cmH₂O) and held airway pressures (5 cmH₂O) constant during microscopy.

Alveolar microinfusion. To load the alveolar epithelium with fluorescent dyes or Abs, we micropunctured single alveoli with glass micropipettes (tip diameter 3-5 μ m) and microinfused ~10 neighboring alveoli^{1,4}. After the microinfusions, the free liquid in the alveolar lumen drained in seconds re-establishing air-filled alveoli⁴. This rapid clearance indicates that the

micropuncture does not rupture the alveolar wall, and that the micropunctured membrane rapidly reseals as reported for other cells⁵. We selected non-micropunctured alveoli for imaging.

Alveolar immunofluorescence. To detect immunofluorescence in live alveoli, we gave alveoli successive 10-minute microinfusions of 4% paraformaldehyde and 0.1% triton X-100. Then, we microinfused fluorescence (Alexa Fluor 488 or 633)-conjugated Abs (40 ng ml^{-1}) for 10 minutes. To washout unbound fluorescence, we microinfused buffer for 10 minutes and commenced imaging after a further 10 minutes. To determine whether the fluorescence was intracellular or extracellular, we microinfused alveoli for 10 minutes with the trypan blue (0.01% solution in PBS).

Lung cell isolation and flow cytometry. To isolate lung cells, we buffer perfused isolated lungs through vascular cannulas to clear blood, and then minced the tissue with scissors. We dissolved the minced tissue in PBS and passed the tissue solution successively through 70 and 40 μm cell strainers (BD Biosciences) and centrifuged the effluent (300 g for 5 min). We treated the resulting pellet and supernatant in three ways. First, to detect BMSCs retained in the lung, we re-suspended the cell pellet in PBS. Then for flow cytometry, we surface stained the cells by incubating the suspension with fluorophore-conjugated Abs (15 min, 4°C). Second, to detect mitochondrial DsRed translocation in AT2 cells, we re-suspended the pellet in PBS. Then to detect intracellular SPB by flow cytometry, we fixed and permeabilized the cells by incubating the suspension sequentially with 4% paraformaldehyde and 0.1% triton X-100. Then we incubated the cells them with Alexa Fluor 488-conjugated Ab against SPB. Third, to detect mBMSC microvesicles in the lung, we centrifuged the supernatant (16,000 g for 15 min) then subjected the resulting supernatant to flow cytometry. We set gating conditions of the flow cytometer (FACScalibur, BD Biosciences) against isotype- and fluorophore-matched IgGs. We analyzed primary data using standard software (FlowJO, Tree Star Inc.).

RNA. To isolate mRNA from alveolar epithelial cells, we intratracheally instilled dispase (1 U ml^{-1} , 2 ml, 45 min) in isolated lungs⁶. Then we carried out the cell isolation procedures, as we describe above, involving tissue mincing, cell straining and centrifugation. We re-suspended the pellet and incubated together with the AT2 cell localizing dye, lysotracker red (LTR)⁷, the nuclear dye, Hoechst 33342 and fluorescence Allophycocyanin (APC)-conjugated Ab against the leukocyte antigen, CD45. Then we processed the suspension in a cell sorter (Influx Cell Sorter, BD Biosciences) to recover AT2 cells and mixed lung cells. We gated the dot plots to exclude cell debris (low forward scatter) and then analyzed for APC and LTR fluorescence. We collected CD45-negative, LTR-positive cells, which also stained for SPB, confirming they were AT2 cells. We also collected alveolar cells which were negative for CD45 and LTR, but positive for Hoechst 33342. Further, we incubated the recovered AT2 and mixed cell populations with FITC-conjugated Abs against CD45 or the BMSC marker, CD90. Absence of FITC fluorescence by flow

cytometry confirmed that these cell populations were free of contamination by leukocytes or instilled BMSCs.

Optical imaging of BMSC nanotubes and microvesicles in alveoli. We defined nanotube formation as a plasma membrane extension of length > 2 μm that contained the cytosolic and mitochondrial fluorescence markers of the parent mBMSC. We defined microvesicles as fluorescent particles of diameter 1-2 μm that lacked fluorescence continuity with the mBMSC cell body.

RNA isolation and PCR analyses. We centrifuged alveolar epithelial cells that we isolated as above and mixed the pellet with 5 volumes of TRIzol (Invitrogen) and stored at -80 °C until use. To extract RNA, we thawed the samples at room temperature and isolated total RNA using the RNeasy Micro Kit (QIAGEN) according to the manufacturer's instructions. We purified the extracted RNA by incubating the samples with DNase (Ambion). We quantified RNA concentration using a NanoDrop ND-1000 spectrophotometer (NanoDrop Technologies Inc.) and converted total RNA from epithelial cell samples into cDNA using the SuperScript® III First-Strand Synthesis SuperMix kit (Invitrogen) according to the manufacturer's instructions. We used the following PCR primers to amplify specific portions of the DNA products: For mouse Cx43, 5'- GAACACGGCAAGGTGAAGAT-3' and 5'- GAGCGAGAGACACCAAGGAC-3'; for Cx40, 5'- CCTGGATACCCTGCATGTCT-3' and 5'- GCTGTCGGATCTTCTCCAG-3'; for Cx37, 5'- TACATGTAGAGCGGGCACTG-3' and 5'- TCTTACACAGCACGCTGACC-3'; for Cx32, 5'- GAAAATGCTACGGCTTGAGG-3' and 5'-CGGAACACCACACTGATGAC-3'; for Cx26, 5'- ATGCTACGACCACCACTTCC-3' and 5'- TACGGACCTTCTGGGTTTTG-3'. The primers for human cytochrome oxidase 1 (*HCO1*) were 5' CGCCACACTCCACGGAAGCA-3' and 5'- CGGGGCATTCCGGATAGGCC-3'; for *HCO2*, 5'- TTCATGATCACGCCCTCATA-3' and 5'- TAAAGGATGCGTAGGGATGG-3'; for mouse cytochrome oxidase 2, 5'- GGCCTACCCATTCCAACCTGGTCT-3' and 5'- CGGCCTGGGATGGCATCAGTTTT-3'; for mouse *Gapdh*, 5'- GGATCTGACGTGCCGCTGG-3' and 5'- CAGCCCCGGCATCGAAGGTG-3'.

We ran the amplified DNA products on 2% agarose gel, and visualized the bands with ethidium bromide.

Immunoblotting and immunoprecipitation. We homogenized samples (Tissue Tearor; Biospec Products) and separated mitochondrial and cytosolic fractions using the mitochondrial isolation kit (Pierce) according to manufacturer's instructions. We determined purity of cell fractionation by immunoblotting for voltage-dependent anion channel (VDAC) in mitochondrial and cytosolic fractions.

To determine endogenous Cx43 expression in mBMSCs expressing mutCx43-GFP, we isolated membrane fractions of mBMSCs using a cell fractionation kit (Pierce) and solubilized them in 2% SDS-containing buffer. To remove mutCx43, we incubated the buffer with beads coated with

anti-GFP mAb (Santa Cruz Biotechnology), centrifuged the sample to remove the beads and then blotted the supernatant with anti-Cx43 Ab (BD Biosciences).

ATP assay in mBMSC lysates. We used our reported methods to quantify ATP concentration in terms of NADPH fluorescence⁸. We incubated mBMSC monolayers with ATP assay buffer for 5 minutes, lysed the cells with 2% triton, then we imaged the supernatant. We normalized NADPH autofluorescence against cell protein content (BCA kit, Pierce) and determined ATP concentration in the supernatant against a calibration curve.

Ca²⁺ determinations. To determine changes in cytosolic Ca²⁺, we loaded mBMSCs with the Ca²⁺ dye, fluo-4 (5 μ M, 40 min). To induce photolytic uncaging of caged Ca²⁺, we co-loaded the cells with fluo-4 and the Ca²⁺ cage, NP-EGTA² (100 nM). To uncage Ca²⁺ from NP-EGTA, we exposed single cells to high-energy UV illumination as we described². We quantified the resulting Ca²⁺ increases by image analyses.

TUNEL staining. We determined cell viability by TUNEL (Terminal deoxynucleotidyl transferase dUTP nick-end labeling) staining with a kit (Roche). For positive control, we incubated mBMSCs with sodium azide (20 mM, 2 h).

Alveolar permeability determinations. To determine alveolar permeability, we used our reported Evans Blue method⁹. We injected Evans Blue-albumin, in a molar ratio of 1 : 4 by the tail vein in mice 4 hours after airway instillation of LPS or PBS. At different time points, we sacrificed the animals and quantified Evans Blue fluorescence in collected bronchoalveolar lavage (BAL) and plasma samples. We express alveolar permeability as a ratio of Evans Blue concentrations in BAL and in plasma.

References

1. Lindert, J., Perlman, C.E., Parthasarathi, K. & Bhattacharya, J. Chloride-dependent secretion of alveolar wall liquid determined by optical-sectioning microscopy. *American journal of respiratory cell and molecular biology* **36**, 688-696 (2007).
2. Parthasarathi, K., *et al.* Connexin 43 mediates spread of Ca²⁺-dependent proinflammatory responses in lung capillaries. *The Journal of clinical investigation* **116**, 2193-2200 (2006).
3. Rowlands, D.J., *et al.* Activation of TNFR1 ectodomain shedding by mitochondrial Ca²⁺ determines the severity of inflammation in mouse lung microvessels. *The Journal of clinical investigation* **121**, 1986-1999 (2011).
4. Wang, P.M., Ashino, Y., Ichimura, H. & Bhattacharya, J. Rapid alveolar liquid removal by a novel convective mechanism. *American journal of physiology. Lung cellular and molecular physiology* **281**, L1327-1334 (2001).
5. Steinhardt, R.A., Bi, G. & Alderton, J.M. Cell membrane resealing by a vesicular mechanism similar to neurotransmitter release. *Science* **263**, 390-393 (1994).
6. Corti, M., Brody, A.R. & Harrison, J.H. Isolation and primary culture of murine alveolar type II cells. *Am J Respir Cell Mol Biol* **14**, 309-315 (1996).
7. Ashino, Y., Ying, X., Dobbs, L.G. & Bhattacharya, J. [Ca²⁺]_i oscillations regulate type II cell exocytosis in the pulmonary alveolus. *American journal of physiology. Lung cellular and molecular physiology* **279**, L5-13 (2000).
8. Corriden, R., Insel, P.A. & Junger, W.G. A novel method using fluorescence microscopy for real-time assessment of ATP release from individual cells. *American journal of physiology. Cell physiology* **293**, C1420-1425 (2007).
9. Conhaim, R.L., Watson, K.E., Spiegel, C.A., Dovi, W.F. & Harms, B.A. Bacteremic sepsis disturbs alveolar perfusion distribution in the lungs of rats. *Critical care medicine* **36**, 511-517 (2008).